Dyes and Pigments 89 (2011) 56–62

Contents lists available at ScienceDirect

Dyes and Pigments

journal homepage: www.elsevier.com/locate/dyepig

# Synthesis of blue light emitting bis(triphenylethylene) derivatives: A case of aggregation-induced emission enhancement

Xiqi Zhang, Zhenguo Chi*, Bingjia Xu, Haiyin Li, Zhiyong Yang, Xiaofang Li, Siwei Liu, Yi Zhang, Jiarui Xu*

*PCFM Lab and DSAPM Lab, OFCM Institute, State Key Laboratory of Optoelectronic Materials and Technologies, School of Chemistry and Chemical Engineering, Sun Yat-sen University, Guangzhou 510275, China*

ARTICLE INFO

*Article history:*
Received 29 March 2010
Received in revised form
18 August 2010
Accepted 9 September 2010
Available online 18 September 2010

*Keywords:*
Aggregation-induced emission enhancement
High glass transition temperature
Blue light emission
Bis(triphenylethylene) derivatives
Device
Synthesis

ABSTRACT

A series of new aggregation-induced emission enhancement derivatives from bis(triphenylethylene) with strong blue-light-emitting properties and high thermal stability have been synthesized. Their maximum fluorescence emission wavelengths range between 464–468 nm, with fluorescence quantum yields of 0.58–0.88. Their glass transition temperatures range from 125 °C to 178 °C. The obtained experimental results demonstrate the different aggregation-induced emission enhancement phenomena caused by the effect of solvent and formation of both H- and J- aggregation states. An emitting device was fabricated using a bis(triphenylene) derivative in the emitting layer which exhibited a luminance efficiency of up to 2 cd/A with a maximum brightness of 548 cd/m$^2$.



## 1. Introduction

In the past decade, organic luminophores have become of great value to the fields of physiology, chemical engineering and display technology due to their applications as biological probes, chemical sensors, and organic light-emitting diodes [1–4]. However, problems related to the production of blue light-emitting materials with strong brightness, long lifetimes and high glass transition temperatures ($T_g$) have suppressed their application on an even wider scale.

Most luminescent materials exhibit relatively weak emissions in the solid state due to the aggregation of molecules leading to the formation of excimers, which results in emission quenching [5,6]. Thus, considerable effort has been exerted in the search for methods to either suppress the quenching of organic luminophores or to produce significant enhancements in their light emission upon aggregation. In line with this, two novel processes have been identified: (1) aggregation-induced emission enhancement (AIEE) and (2) aggregation-induced emission (AIE) [7–13]. AIEE (or AIE) materials have been found to be promising emitters in the fabrication of electroluminescent devices with high efficiency and stimuli-responsiveness for use in multifunctional switches [14,15].

The $T_g$ temperature of an organic luminophore is one of the important factors influencing the stability and lifetime of a device. If a device is heated above the $T_g$ of the organic luminophore, irreversible failure can occur.

In aggregates, strong clustering of aromatic chromophores is often observed with the spectral shift of a maximum absorption band. In aromatic moieties, the blue shift is usually assigned to the parallel head-to-head alignment of aromatic chromophores, also referred to as H-aggregation. In contrast, a red shift is normally observed when chromophores are aggregated in a head-to-tail manner, which is referred to as J-aggregation. The aggregation state of aromatic chromophores can greatly influence the morphologies of the formed aggregates, as well as their absorption and fluorescence spectra [16–19].

We have already reported a new class of triphenylethylene carbazole derivatives that display strong blue light emissions, high $T_g$ temperatures and AIE effects [20]. For comparison, in this work a new class of bis(triphenylethylene) derivatives were synthesized. These derivatives also show strong blue light emissions and high $T_g$ temperatures, but unlike their earlier counterparts, they are AIEE-active. It is expected that these novel compounds can be used as potential materials for blue-light emitters in luminescent devices.

* Corresponding authors. Tel.: +86 20 84112712; fax: +86 20 84112222.
*E-mail addresses:* chizhg@mail.sysu.edu.cn (Z. Chi), xjr@mail.sysu.edu.cn (J. Xu).

0143-7208/$ – see front matter © 2010 Elsevier Ltd. All rights reserved.
doi:10.1016/j.dyepig.2010.09.003

## 2. Experimental

### 2.1. Materials and measurements

All reagents and chemicals were purchased from Alfa-Aesar Ltd. and used as received. Analytical grade DMF was purified by distillation under an inert nitrogen atmosphere. Tetrahydrofuran (THF) was distilled from sodium/benzophenone. Ultra-pure water was used in the experiments. All other solvents as analytical grade were purchased from Guangzhou Dongzheng Company and used without further purification. The intermediates **1** and **2** were prepared according to the literature methods [20,21], and **3** was obtained in a similar manner. 1,4-Bis(diethoxyphosphinylmethyl) benzene was synthesized according to the literature method starting from 4,4′-bis(bromomethyl)biphenyl [22]. Aliquat 336 (tricaprylylmethylammonium chloride) used as phase transfer agent in the Suzuki reaction is both harmful and an irritant, may cause irreversible damage to the eyes and is also toxic to aquatic organisms leading to potential long term adverse effects to the aquatic environment. Be careful to use it.

$^1$H-NMR was measured on a Varian Mercury-Plus 300 spectrometer with chemical shifts reported as ppm (in $CDCl_3$ or DMSO-$d_6$, TMS as internal standard). Mass spectra were measured on a Thermo MAT95XP-HRMS spectrometer. Elemental analyses were performed with an Elementar Vario EL Elemental Analyzer. UV–Vis absorption spectra (UV) were recorded on a Hitachi UV–Vis spectrophotometer (U-3900). Fluorescence spectra (PL) were determined with a Shimadzu RF-5301PC spectrometer and the slit widths were 1.5 nm for excitation and 3.0 nm for emission. To measure the PL spectra in thin-layer chromatography (TLC) plates, aluminum TLC plates (Merck, Silica 60 F254) were used. The samples in TLC plates were prepared and determined according to the literature [9]. The fluorescence quantum yields ($\Phi_{FL}$) were measured by the standard optically diluted method in degassed dichloromethane solutions (ca. $10^{-5}$ M) using 9,10-diphenylanthracene ($\Phi_{FL} = 0.90$, in dichloromethane) as a reference standard [23]. Differential scanning calorimetry (DSC) curves were obtained with a TA thermal analyzer (Q10) at a heating rate of 10 °C/min under $N_2$ atmosphere. Thermogravimetric analyses (TGA) were performed with a TA thermal analyzer (A50) under $N_2$ atmosphere with a heating rate of 20 °C/min. The sizes of the particles of the compounds in THF/water mixtures were determined using a ZetaPALS dynamic light scattering system (Brookhaven, ZetaPALS Zeta Potential Analyzer).

Cyclic voltammetry (CV) measurements were carried out on a Shanghai Chenhua electrochemical workstation (CHI660C) in a three-electrode cell with a Pt disk working electrode, an Ag/AgCl reference electrode, and a glassy carbon counter electrode. All CV measurements were performed under an inert argon atmosphere with supporting electrolyte of 0.1 M tetrabutylammonium perchlorate (n-$Bu_4NClO_4$) in dichloromethane at scan rate of 100 mV/s using ferrocene as standard. The HOMO energy levels were obtained using the onset oxidation potentials from the CV curves. The lowest unoccupied molecular orbital/highest occupied molecular orbital (LUMO/HOMO) energy gaps $\Delta Eg$ for the compounds were estimated from the onset absorption wavelengths of the UV absorption spectra.

#### 2.1.1. Device fabrication and measurement

The glass substrate pre-coated with indium-tin-oxide (ITO) was cleaned by an ultrasonic bath of acetone, ethanol and deionized water, and then dried in an oven at 80 °C. Surface treatment was carried out by exposing ITO to UV-ozone plasma. The electroluminescence (EL) device was fabricated as follows. The hole-transporting layer, a 50 nm thick film of 4,4′-bis(1-naphthylphenylamino) biphenyl (NPD) was deposited on the ITO surface by high vacuum thermal evaporation. Compound **$C_4$** (30 nm thick layer) was evaporated on the NPD layer and a 20 nm thick 8-hydroxyquinoline aluminum ($Alq_3$) layer was then deposited as the electron transporting layer. Finally LiF (1 nm) and Al (100 nm) were deposited on top of the organic layers by thermal evaporation. The fabricated multilayer organic light emitting devices possessed the structure of ITO/NPB (50 nm)/Sample(30 nm)/$Alq_3$(20 nm)/LiF (1 nm)/Al (100 nm). Each layer was deposited at $>10^{-5}$ Pa with BOC Edwards Auto 500 box chamber system. The thickness of layer was taken by Dektak 6 M profilometer (Veeco). EL spectrum at 10 V electric voltage was recorded using F-4500 fluorescence spectrometer (Hitachi). The current-voltage-luminance characteristics were determined in ambient atmosphere using a Matrix DC power supply MPS-3002L-3 (Matrix Technology Inc, China) and a Minolta LS-110 meter (Konica Minolta Sensing, Japan). The currents were determined by UNI-T (UT71 series) intelligent digital multimeter (Uni-Trend Group Limited, Hongkong).

### 2.2. Preparation of aggregates [24]

Stock THF solutions of the synthesized compounds with a concentration of 0.1 mM were prepared. 1 mL of this stock solution was transferred to a 10 mL volumetric flask. After adding an appropriate amount of THF, Ultra-pure water was added dropwise under ultrasound treatment to prepare a 10 μM solution in a THF/$H_2O$ mixture with a specific water fraction. Absorption and emission spectra of the resulting solutions and aggregates were measured immediately after the sample preparation.

### 2.3. Synthesis of intermediate **3**

A solution of dibiphenyl-4-ylmethanone 3.3 g (10 mmol) and diethyl 4-bromobenzylphosphonate 3.1 g (10 mmol) in anhydrous tetrahydrofuran (40 mL) was stirred under a $N_2$ atmosphere at 0 °C. Postassium tert-butoxide 1.1 g (10 mmol) was added quickly and the mixture was stirred continuously for 2 h at room temperature. The reaction mixture was precipitated into ethanol. The precipitate obtained was filtered, and washed with ethanol three times to afford 3.9 g product as a white powder (80% yield). $^1$H NMR (300 MHz, DMSO-$d_6$) $\delta$: 7.70–7.59 (m, 6H), 7.59–7.55 (d, 2H), 7.51–7.46 (d, 2H), 7.46–7.40 (d, 4H), 7.40–7.34 (m, 2H),7.32–7.26 (m, 4H), 7.00–6.96 (d, 2H), 6 .95 (s, 1H); MS (EI), *m/z*: 486 ($[M]^+$, calcd for $C_{32}H_{23}Br$, 486); Anal. calc. for $C_{32}H_{23}Br$: C, 78.85; H, 4.76; Br, 16.39 Found: C, 78.79; H, 4.72.

### 2.4. Synthesis of ***$C_2B$***

To a stirred solution of **2** (6.0 g, 9.0 mmol) in anhydrous THF (100 mL) was added *n*-butyllithium solution in hexane (2.2 M, 6 mL, 13.2 mmol) dropwise slowly at −78 °C. The mixture was stirred at -78 °C under Ar gas for an additional 5 h. $B(OCH_3)_3$ (2.2 mL) was added quickly at −78 °C and the mixture was stirred overnight allowing the temperature to rise gradually to room temperature. Water (40 mL) was added and then acidified with concentrated HCl. The mixture was stirred for a further 2 h. The product was extracted into ethyl acetate (3 × 50 mL). The organic layer was separated and dried over anhydrous sodium sulfate. After removing the solvent under reduced pressure, the residue was chromatographed on a silica gel column with acetone/dichloromethane (1:20 by volume) as eluent to give **$C_2B$** (2.1 g, 55% yield). $^1$H NMR (300 MHz, DMSO-$d_6$) $\delta$: 7.14 (s, 1 H, >C═CH–), 7.25–7.58 (m, 16 H), 7.62–7.78 (m, 8 H), 7.98 (s, 2 H, -$B(OH)_2$), 8.20–8.30 (m, 4 H, carbazole-H); MS (EI), *m/z*: 586 ($[M\text{-}(B(OH)_2)]^+$, calcd for $C_{44}H_{29}$, 585); Anal. calc. for $C_{44}H_{31}BN_2O_2$: C, 83.81; H, 4.96; N, 4.44 Found: C, 83.64; H, 4.89; N, 4.48.

### 2.5. Synthesis of $C_2B_2$

1-Bromo-4-(2,2-di(biphenyl)ethenyl)benzene (**3**) (0.20 g, 0.41 mmol) and **$C_2B$** (0.31 g, 0.49 mmol) were dissolved in the mixture of toluene (30 mL), tricaprylylmethylammonium chloride (Aliquat 336) (5 drops) and 2 M potassium carbonate aqueous solution (8 mL). The mixture was stirred at room temperature for 0.5 h under Ar gas followed adding $Pd(PPh_3)_4$ (0.010 g, $8.70 \times 10^{-3}$ mmol) and then heated to 90 °C for 24 h. After that the mixture was poured into water and extracted three times with ethyl acetate. The organic layer was dried over anhydrous sodium sulfate. After removing the solvent under reduced pressure, the residue was chromatographed on a silica gel column with *n*-hexane/dichloromethane (2:1 by volume) as eluent to give **$C_2B_2$** (0.20 g, 49% yield). $^1$H NMR (300 MHz, $CDCl_3$) $\delta$: 7.08 (s, 1 H,>C═CH−), 7.16 (s, 1 H,>C═CH−), 7.18−7.24 (m, 4 H), 7.27−7.39 (m, 8 H), 7.40−7.71 (m, 34 H), 8.16 (d, 4 H, $J = 7.8$ Hz, carbazole-H); MS (EI), *m/z*: 992 ($[M]^+$, calcd for $C_{76}H_{52}N_2$, 992); Anal. calc. for $C_{88}H_{58}N_4$: C, 91.90; H, 5.28; N, 2.82 Found: C, 91.73; H, 5.23; N, 2.90.

### 2.6. Synthesis of $C_4$

1,4-Bis(diethoxyphosphinylmethyl)benzene (0.90 g, 2.0 mmol) and **1** (2.6 g, 5.0 mmol) were dissolved in THF (60 mL), then *t*-BuOK (0.56 g) was added under Ar gas. The solution was stirred at room temperature overnight. After removing the solvent under reduced pressure, the residue was recrystallized with THF/EtOH to give **$C_4$** (1.7 g, 75% yield). $^1$H NMR (300 MHz, $CDCl_3$) $\delta$: 7.24 (s, 2 H, >C═CH−), 7.25−7.35 (m, 12 H), 7.43−7.48 (m, 8 H), 7.52−7.55 (m, 12 H), 7.58−7.72 (m, 16 H), 8.18 (d, 8 H, $J = 8.0$ Hz, carbazole-H); MS (FAB), *m/z*: 1171 ($[M+H]^+$, calcd for $C_{88}H_{58}N_4$, 1171); Anal. calc. for $C_{88}H_{58}N_4$: C, 90.23; H, 4.99; N, 4.78. Found: C, 90.04; H, 4.70; N, 5.01.

### 2.7. Synthesis of $B_4$

1,4-Bis(diethoxyphosphinylmethyl)benzene (0.20 g, 0.44 mmol) and 4,4′-diphenylbenzophenone (0.37 g, 1.1 mmol) were dissolved in THF (20 mL), then t-BuOK (0.20 g) was added under Ar gas. The solution was stirred at room temperature overnight. After removing the solvent under reduced pressure, the residue was chromatographed on a silica gel column with *n*-hexane/dichloromethane (2:1 by volume) as eluent to give **$B_4$** (0.10 g, 28% yield). $^1$H NMR (300 MHz, $CDCl_3$) $\delta$: 7.06 (s, 2 H,>C═CH−), 7.09-7.17 (d, 4 H, $J = 8.4$ Hz), 7.30−7.51 (m, 24 H), 7.54−7.69 (m, 16 H); MS (EI), *m/z*: 814 ($[M]^+$, calcd for $C_{64}H_{46}$, 814); Anal. calc. for $C_{64}H_{46}$: C, 94.31; H, 5.69 Found: C, 94.47; H, 5.63.

## 3. Results and discussion

### 3.1. Synthesis

As illustrated in Scheme 1, ketone **1** was converted into the triarylethene **2** using Wadsworth-Emmons chemistry as previously described starting from carbazole [20,21]. The related bis(biphenyl) bromoarylethene **3** was obtained in a similar manner starting from dibiphenyl-4-ylmethanone. **$C_2B_2$** was constructed using the palladium (Pd)-catalyzed Suzuki coupling reaction of **3** with the intermediate compound **$C_2B$**, which was prepared from **2**, *n*-BuLi and B $(OCH_3)_3$.

Compound **$C_4$** was synthesized via the Wittig−Horner reaction of intermediate **1** and 1,4-bis(diethoxyphosphinylmethyl)benzene. Although **$C_4$** has appeared in two patents [25,26], to the best of our knowledge, the properties of the compound have not been well studied, especially the AIEE properties. Compound **$B_4$** was prepared from 1,4-bis(diethoxyphosphinylmethyl) benzene and 4,4′-diphenylbenzophenone under the same reaction conditions (Scheme 2).

### 3.2. Thermal properties

The thermal and photophysical properties of the synthesized compounds **$C_4$**, **$C_2B_2$** and **$B_4$** are summarized in Table 1. The thermal properties were investigated by TGA and DSC. As can be seen from Table 1 and Fig. S1, relatively high $T_g$ temperatures ranging from 125 to 178 °C were observed. These $T_g$ values were much higher than those reported for 4,4′-bis(2,2-diphenylvinyl)-1,1′-biphenyl (DPVBi, Scheme 2) (64 °C) [27], which might be attributed to the combined presence of the carbazolyl and phenyl substituent groups in the synthesized derivatives. It was also observed that the $T_g$ of the compound containing four carbazolyl groups (**$C_4$**) was higher than that of the corresponding compound containing two carbazolyl

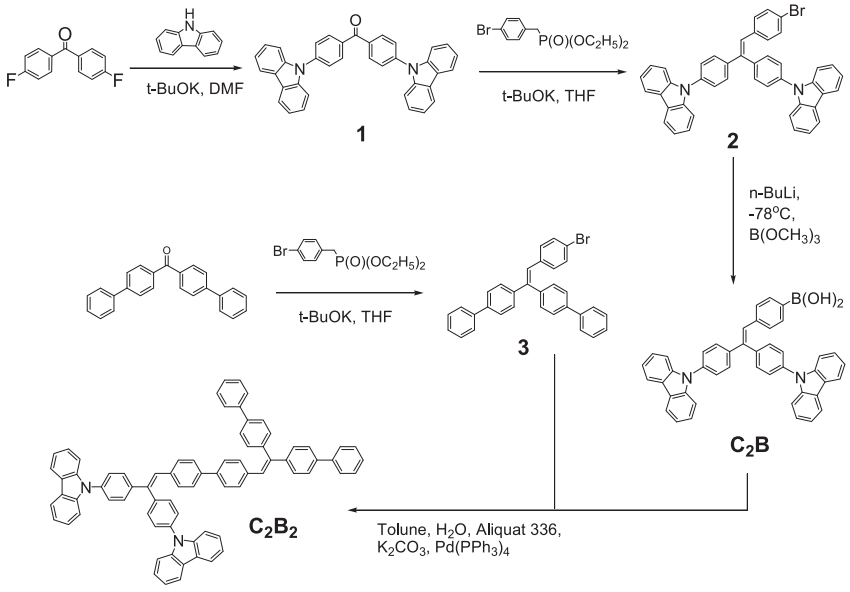


**Scheme 1.** Synthetic routes of **$C_2B_2$**.

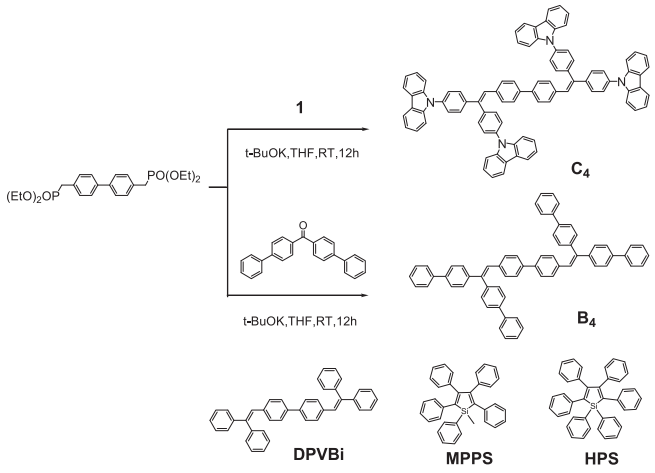


**Scheme 2.** Synthetic routes of $\mathbf{C_4}$ and $\mathbf{B_4}$, and the structures of DPVBi, MPPS and HPS.

groups and two phenyl groups ($\mathbf{C_2B_2}$), which in turn was higher than that of the compound containing four phenyl groups ($\mathbf{B_4}$). It is well-known that carbazole group possesses a bulky rigid planar molecular structure, which helps to effectively decrease rotation and increase thermal stability. Thus, the differences in $T_g$ of these compounds were attributed to the introduction of carbazolyl groups.

It is interesting to note that the melting-point temperatures ($T_m$) of compounds $\mathbf{C_4}$ and $\mathbf{B_4}$ could be obtained by DSC at 363 °C and 298 °C, respectively (Fig. S2). However, no melting point could be observed for $\mathbf{C_2B_2}$ using DSC. The reason is that the asymmetric structure of $\mathbf{C_2B_2}$ influences the molecular tight packing in the solid state, thus forming an amorphous structure.

The thermal decomposition temperatures ($T_d$) of these compounds (corresponding to 5% weight loss under $N_2$ atmosphere) were in the range of 468–535 °C (Table 1 and Fig. S3). The $T_d$ values of the compounds were higher than those of the reported AIEE-active compounds, 1-methyl-1,2,3,4,5-pentaphenylsilole (MPPS, see Scheme 2) (309 °C) and 1,1,2,3,4,5-hexaphenylsilole (HPS, see Scheme 2) (351 °C) [28]. The results indicate that the compounds have very high levels of thermal stability. The thermal stability of organic compounds is critical to the stability and lifetime of photoelectric devices. Thus, the high level of thermal stability would be beneficial if the compounds were to be used in photoelectric materials.

### 3.3. Photophysical and electrochemical properties

The maximum UV absorption wavelengths of the compounds were ca. 367 nm in dichloromethane and their maximum PL emission wavelengths in cyclohexane and dichloromethane solutions appeared at ca. 463 nm and at ca.467 nm, respectively (Table 1, Fig. S4). Despite the difference of the substituents in compounds $\mathbf{C_4}$, $\mathbf{C_2B_2}$ and $\mathbf{B_4}$, the maximum absorption wavelengths and the maximum emission wavelengths of these compounds were very similar in solution. In comparison to the data recorded in dilute solutions, the maximum emission wavelengths of the compounds on TLC plates were very close to those in solutions. However, the maximum emission wavelengths of compounds in powder states were significantly red-shifted compared to those determined for solutions and on TLC plates (Fig. S5).

**Table 1**
Thermal and photophysical properties of the compounds.

| Compd | $T_g$ (°C) | $T_m$ (°C) | $T_d$ (°C) | $\lambda_{max}^{abs}$ [a] (nm) | $\lambda_{max}^{em}$ (nm) | | | | $\phi_{FL}$ [e] |
|---|---|---|---|---|---|---|---|---|---|
| | | | | | MC[a] | CH[b] | TLC[c] | Powder[d] | |
| $\mathbf{C_4}$ | 178 | 363 | 535 | 368 | 462 | 466 | 464 | 479 | 0.58 |
| $\mathbf{C_2B_2}$ | 149 | NA | 493 | 367 | 464 | 467 | 465 | 490 | 0.75 |
| $\mathbf{B_4}$ | 125 | 298 | 468 | 368 | 464 | 468 | 468 | 496 | 0.88 |

[a] Measured in dichloromethane solution.
[b] Measured in cyclohexane solution.
[c] Measured in TLC plate.
[d] Measured in powder state.
[e] Fluorescence quantum yields, measured in cyclohexane solution using 9,10-diphenylanthracene ($\phi_{FL(ref)} = 0.90$, in dichloromethane) as standard, excited at 365 nm.

As shown in Fig. 1, a decreasing trend can be observed in the absorption of $\mathbf{C_4}$ to $\mathbf{C_2B_2}$ to $\mathbf{B_4}$ at 344 nm. The molar absorption coefficients (ε) of $\mathbf{C_4}$, $\mathbf{C_2B_2}$ and $\mathbf{B_4}$ at 344 nm are $1.426 \times 10^5$, $1.171 \times 10^5$ and $0.817 \times 10^5$ L mol$^{-1}$ cm$^{-1}$ in dichloromethane. The disappearance of 344 nm absorption peak in the UV spectrum of compound $\mathbf{B_4}$ indicates that the 344 nm wavelength corresponds to the absorption of carbazolyl groups. As the number of carbazolyl groups for $\mathbf{C_4}$, $\mathbf{C_2B_2}$ and $\mathbf{B_4}$ decreased from four to two to zero, the absorption at 344 nm gradually weakened.

The fluorescence quantum yields ($\Phi_{FL}$) were determined using 9,10-diphenylanthracene as a standard. It was observed that the compounds had rather high quantum yields, and the $\Phi_{FL}$ values ranged from 0.58 to 0.88. The $\Phi_{FL}$ values increased with the decrease of carbazolyl groups.

Cyclic voltammetry (CV) analyses were carried out to measure the HOMO values of the synthesized compounds. According to the CV data, the HOMO levels of compounds $\mathbf{C_4}$, $\mathbf{C_2B_2}$ and $\mathbf{B_4}$ were 5.21 eV, 5.31 eV and 5.60 eV, respectively. These results indicate that the increase in the number of carbazolyl groups decreases the HOMO level of the molecule and lowers the barrier to hole injection from the most widely used anode material, indium tin oxide (ITO), which has a work function of 5.0 eV. The energy band gaps of the compounds were estimated by analyzing absorption edge with a plot of UV curve. The band gaps of $\mathbf{C_4}$, $\mathbf{C_2B_2}$ and $\mathbf{B_4}$ were found to be 2.98 eV, 2.96 eV and 2.93 eV, respectively. The LUMO levels of $\mathbf{C_4}$, $\mathbf{C_2B_2}$ and $\mathbf{B_4}$ calculated by HOMO- $E_g$ were 2.23, 2.35 and 2.67 eV, respectively.

### 3.4. AIEE properties

To determine whether these three new compounds are AIEE active, the fluorescence behaviour of their diluted mixtures was studied in a mixture of water/THF under different water fractions.

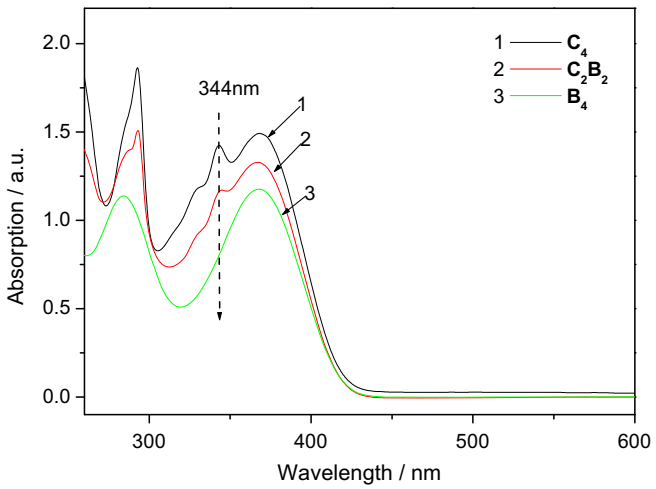


**Fig. 1.** UV spectra of $\mathbf{C_4}$, $\mathbf{C_2B_2}$, and $\mathbf{B_4}$ in dichloromethane solutions.

Since the compounds were insoluble in water, increasing the water fraction in the mixed solvent could change their existing forms from a solution or well-dispersed state in THF to the aggregated particles in the aq. THF with a high water content.

Changes in the PL peak intensities versus water fraction of the mixture for compound **$C_4$** were plotted, as shown in Fig. 2 as an example. When the water fraction was increased from 0% to 80%, the fluorescence intensity of **$C_4$** was correspondingly enhanced 4.7-fold. Similar enhancement was observed in the behaviour of the remaining two compounds (Figs. S6 and S7). When the water fraction was increased from 0% to 80%, the fluorescence intensities of **$C_2B_2$** and **$B_4$** were enhanced 4.2-fold and 2.3-fold, respectively. This increase in fluorescence intensity was considered to be a result of the AIEE effect. As aggregates formed the restriction of intermolecular rotation increased which led to increased fluorescence emission. The results indicate that the AIEE effects of the compounds increased along with increases in the number of carbazolyl groups that were present in the molecules.

As can be seen, after reaching a maximum intensity at 60% (for **$C_4$** and **$C_2B_2$** systems) or 80% (for **$B_4$** system) $H_2O$ content the PL intensity of the three compounds decreases with increasing water content. This phenomenon was often observed in some compounds with AIEE properties, but the reasons remain unclear. There are two possible explanations for this phenomenon: 1) after the aggregation, only the molecules on the surface of the nanoparticles emitted light and contributed to the fluorescent intensity upon excitation, leading to a decrease in fluorescent intensity. However, the restriction of intramolecular rotations of the aromatic rings around the carbon-carbon single bonds in the aggregation state could enhance light emission. The net outcome of these antagonistic processes depends on which process plays a predominant role in affecting the fluorescent behaviour of the aggregated molecules [29]; 2) when water is added, the solute molecules can aggregate into two kinds of nanoparticle suspensions: crystal particles and amorphous particles. The former leads to an enhancement in the PL intensity, while the latter leads to a reduction in intensity [20]. Thus, the measured overall PL intensity data depends on the combined actions of the two kinds of nanoparticles. However, it is hard to control the formation of nanoparticles in high water content. Thus, the measured PL intensity often shows no regularity in high water content.

It is noteworthy that the diameters of the particles of the compounds formed in the water/THF mixtures measured by dynamic light scattering correlate with the water/THF ratio (Fig. 3, Table S1). When the water fraction was up to 60%, the particles with dimensions in the micro- or nano-scale could be detected. With the further increasing proportion of water, the effective diameter of the particles decreased (For example, for compound **$C_4$**, water/THF 60:40, 1131 nm; 70:30, 362 nm; 80:20, 356 nm; 90:10, 240 nm). It is also important to note, from the dynamic light scattering measurements, that the nanoparticles could not form when the water/THF ratio is lower than 60:40. This ratio is close to the ratio that the PL emission intensity abruptly enhanced.

The absorption spectra of the compounds in the water/THF mixtures (10 μM) are shown in Fig. 4, Figs. S8 and S9. The spectral profile was significantly changed when >50% water was added to the THF solution. The entire spectrum started to increase in absorption, indicating the formation of nanoscopic aggregates of the compounds. The light scattering, or Mie effect, of the nano-aggregates suspensions in the solvent mixtures effectively decreased light transmission in the mixture and caused the apparent high absorbance and level-off tail in the visible region of the UV absorption spectrum [30,31].

With increasing water content, the maximum absorption bands of **$B_4$** showed blue shifts, indicating the formation of H-aggregates [16]. However, under the same condition, the maximum absorption bands of **$C_4$** and **$C_2B_2$** showed red shifts, suggesting the formation of J-aggregates. When the water fraction in the solvent increased from 0% to 90%, the UV absorption wavelength of **$B_4$** blue-shifted from 370 nm to 359 nm (an 11-nm blue shift), while **$C_4$** and **$C_2B_2$** showed red shifts from 370 nm to 402 nm (a 32-nm red shift) and from 368 nm to 376 nm (an 8-nm red shift), respectively. The H-aggregates of **$B_4$** and J-aggregates of **$C_4$** and **$C_2B_2$** may have been derived from the molecular architecture of the above-mentioned compounds, which could influence the aggregation state in two aspects: (1) The distance of the adjacent molecules decreased with the increase of phenyl groups and decrease of carbazolyl groups in the compounds, respectively; (2) The twisted structure of **$C_4$** and **$C_2B_2$** prevented face-to-face π–π stacking interactions along the long molecular axis by the bulky carbazolyl groups, which tended to favor J-aggregation instead of H-aggregation in the solid state (Fig. 5). Due to the difference of number of carbazolyl groups in **$C_4$** and **$C_2B_2$**, the steric hindrance effects would result in differences in molecular spatial structures, then affect their aggregation states.

It could be seen from the PL spectra of **$C_4$**, **$C_2B_2$** and **$B_4$** in THF with varying amounts of water when the water fraction was

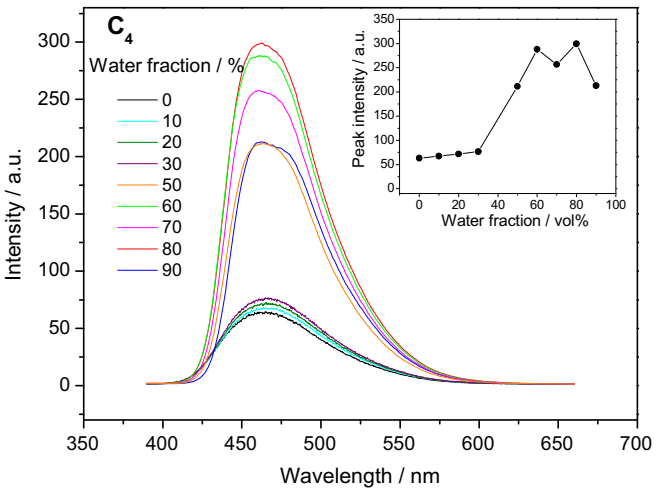


**Fig. 2.** PL spectra of **$C_4$** (10 μM) in THF with varying amounts of water (% fraction of volume) (The inset depicts the changes of PL peak intensiy with water fraction).

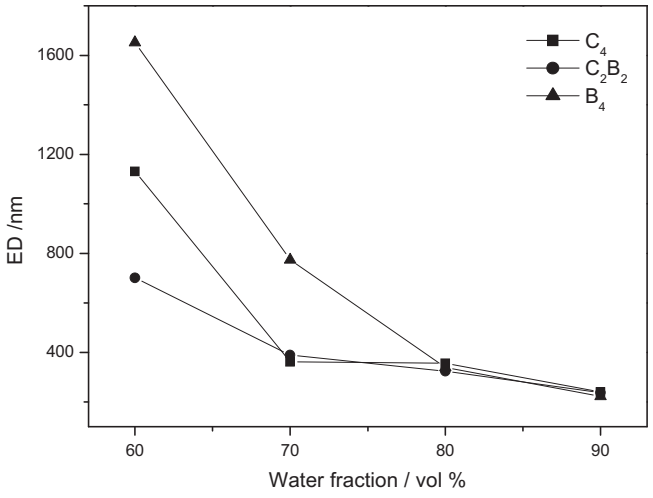


**Fig. 3.** Effective diameter (ED) determined by dynamic light scattering of the compounds (10 μM) in water/THF mixtures as a function of water fraction.

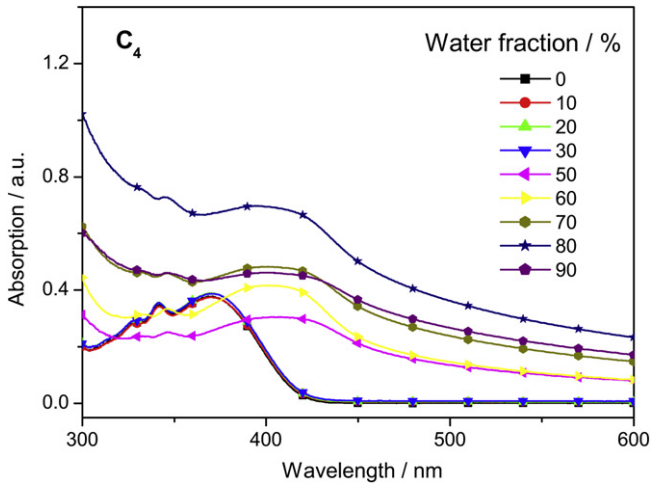


**Fig. 4.** UV spectra of $\mathbf{C_4}$ (10 μM) in THF with varying amounts of water (% fraction of volume).

increased from 0% to 90%, the PL emission wavelength of $\mathbf{C_4}$ was maintained; meanwhile, $\mathbf{C_2B_2}$ and $\mathbf{B_4}$ exhibited 2-nm red shift and a 13-nm red shift changes, respectively. This phenomenon may have also been derived from two aspects: (1) the aggregation state of the compounds and (2) the influence of the solvent effect. As the water fraction increases in the mixed solvents, $\mathbf{C_4}$ and $\mathbf{C_2B_2}$ may form J-aggregates, while $\mathbf{B_4}$ may form H-aggregates. As we know, the formation of J-aggregates could cause the fluorescence wavelength to blue-shift, while the formation of H-aggregates could cause the same to red-shift [32]. The fluorescence wavelength could also be red-shifted by increases in solvent polarity, such as those caused by increasing water fractions. For $\mathbf{C_4}$, the influences of aggregation and the solvent effect may counteract each other such that the fluorescence wavelength is maintained and unchanged. The solvent effect appears to have dominated in the compounds $\mathbf{C_2B_2}$ and $\mathbf{B_4}$, and thus, their fluorescence wavelengths have red-shifted. It was also observed that when the water fraction in $\mathbf{C_2B_2}$ was increased to 80%, a new PL band appeared in the region of shorter wavelength, indicating the formation of J-aggregation (Fig. S6).

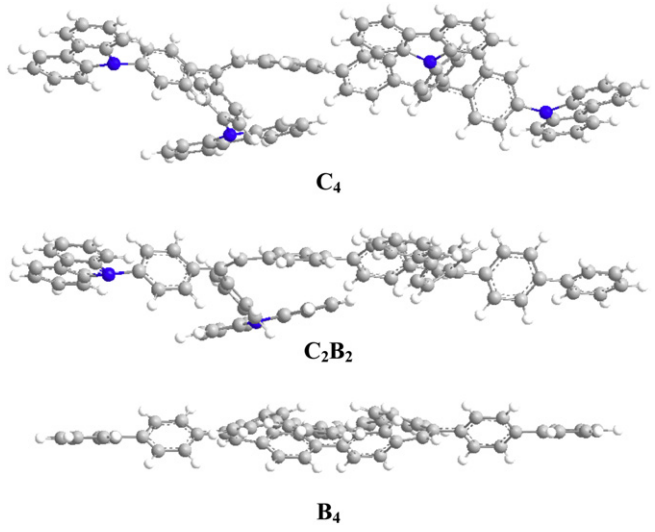


**Fig. 5.** Molecular models of the energy minimized structures of $\mathbf{C_4}$, $\mathbf{C_2B_2}$, and $\mathbf{B_4}$ (simulated by Chem 3D Ultra 8.0).

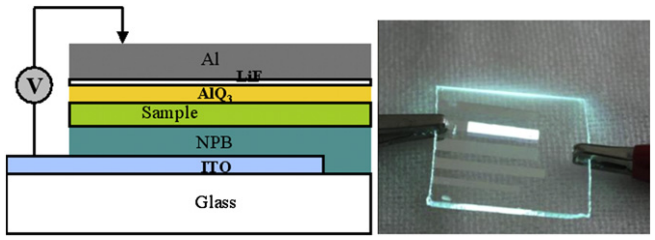


**Fig. 6.** OLED device configuration (left) and the image of the device taken at 10 V voltage (right).

### 3.5. Device fabrication and electroluminescence properties

The strong blue light emission and high thermal stability of the compounds prompted us to use them to construct electroluminescence (EL) devices. As an example, a multilayer electroluminescence device, ITO/NPB (50 nm)/Sample(30 nm)/$Alq_3$(20 nm)/LiF (1 nm)/Al(100 nm), was fabricated using vapor deposition processes. 4,4′-Bis(1-naphthylphenylamino)biphenyl (NPB) was used as the hole-transporting layer, and sample $\mathbf{C_4}$ as the emitting layer, 8-hydroxyquinoline aluminum ($Alq_3$) as the electron-transporting layer. LiF was used between the electron-transporting layer and cathode Al to enhance electron injection, and indium-tin oxide (ITO) coated glass was used as the substrate and anode. The configuration and the image taken at 10 V voltage of the OLED device is shown in Fig. 6.

The current–voltage-luminance characteristics of the unoptimized device is presented in Fig. 7. The turn-on voltage, which is defined as the voltage when the luminance is 1 cd/m$^2$, was 6.0 V. The device exhibited a good light-emitting property in which its luminance efficiency can reach up to 2 cd/A with a maximum brightness of 548 cd/m$^2$.

The EL spectrum of the device is shown in Fig. S10. Comparison of the EL spectrum with PL emission spectra of the compound in powder state and in dichloromethane solution showed that the profiles of the EL band and the PL bands were similar with about 8 nm red-shift and 5 nm blue-shift for the EL peak (474 nm) compared with those of the PL peaks in dichloromethane solution (466 nm) and in powder state (479 nm). Extended investigation and further optimization on the electroluminescence devices based on this new series of AIE compounds are being carried out in our laboratory and will be reported in due course.

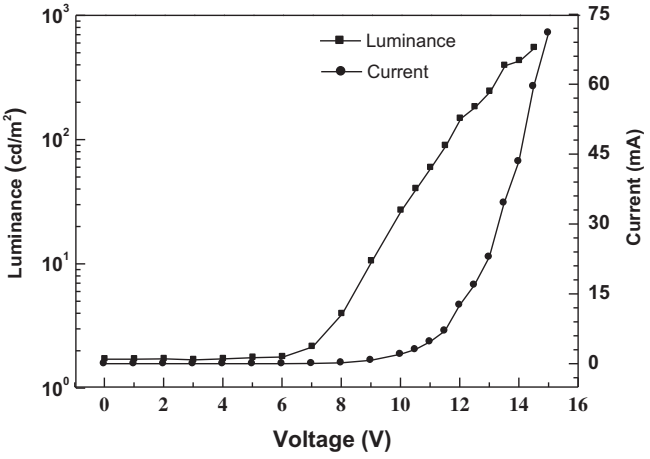


**Fig. 7.** Diagram of luminance and current *vs.* voltage of the OLED device.

## 4. Conclusions

In this work, we have developed further examples of AIEE-active compounds in the form of bis(triphenylethylene) derivatives. These new derivatives showed high levels of thermal stability, with $T_g$ values ranging from 125–178 °C. The derivatives were all categorized as blue-light emitters and their maximum emission wavelengths were in the range of 464–468 nm. The compounds exhibited high fluorescent efficiencies and their fluorescence quantum yields were in the range of 0.58–0.88. The resultant compounds with high $T_g$ values and high fluorescence quantum yield could enable the development and processing of new high-performance organic electronic devices. The HOMO levels of **$C_4$** and **$C_2B_2$** allows their use as materials in OLED devices to lower the barrier of hole injection. The observed AIEE properties demonstrate that the composition of a mixture of THF and water influences the formation of different aggregation states and that the solvent effect contributes to the variation of UV and PL spectra. The device using **$C_4$** as emitting layer exhibited a good light-emitting property in which its luminance efficiency can reach up to 2 cd/A with a maximum brightness of 548 cd/m$^2$.

## Acknowledgements

The authors gratefully acknowledge the financial support from the National Natural Science Foundation of China (Grant numbers: 50773096, 50473020), the Start-up Fund for Recruiting Professionals from “985 Project” of SYSU, the Science and Technology Planning Project of Guangdong Province, China (Grant numbers: 2007A010500001-2, 2008B090500196), Construction Project for University-Industry cooperation platform for Flat Panel Display from The Commission of Economy and Informatization of Guangdong Province (Grant numbers: 20081203) and the Open Research Fund of State Key Laboratory of Optoelectronic Materials and Technologies.

## Appendix. Supplementary data

Supplementary data associated with this article can be found in the online version, at doi:10.1016/j.dyepig.2010.09.003.

## References

[1] Wakamiya A, Mori K, Yamaguchi S. 3-Boryl-2,2′-bithiophene as a versatile core skeleton for full-color highly emissive organic solids. Angewandte Chemie International Edition 2007;46:4273–6.
[2] Citterio D, Takeda J, Kosugi M, Hisamoto H, Sasaki S, Komatsu H, et al. pH-independent pluorescent chemosensor for highly selective lithium ion sensing. Analytical Chemistry 2007;79:1237–42.
[3] McDonagh C, Burke CS, MacCraith BD. Optical chemical sensors. Chemical Reviews 2008;108:400–22.
[4] Ligler FS, Sapsford KW, Golden JP, Shriver-Lake LC, Taitt CR, Dyer MA, et al. The array biosensor: portable, automated systems. Analytical Sciences 2007;23:5–10.
[5] Jenekhe SA, Osaheni JA. Excimers and exciplexes of conjugated polymer. Science 1994;265:765–8.
[6] Friend RH, Gymer RW, Holmes AB, Burroughes JH, Marks RN, Taliani C, et al. Electroluminescence in conjugated polymers. Nature 1999;397:121–8.
[7] Luo JD, Xie ZL, Lam JWY, Cheng L, Chen HY, Qiu CF, et al. Aggregation-induced emission of 1-methyl-1,2,3,4,5-pentaphenylsilole. Chemical Communications; 2001:1740–1.
[8] Yu G, Yin S, Liu Y, Chen J, Xu X, Sun X, et al. Structures, electronic states, photoluminescence, and carrier transport properties of 1,1-disubstituted 2,3,4,5-tetraphenylsiloles. Journal of the American Chemical Society 2005;127:6335–46.
[9] Chen J, Law C, Lam J, Dong Y, Lo S, Williams I, et al. Synthesis, light emission, nanoaggregation, and restricted intramolecular rotation of 1,1-substituted 2,3,4,5-tetraphenylsiloles. Chemistry of Materials 2003;15:1535–46.
[10] Bhongale CJ, Hsu CS. Emission enhancement by formation of aggregates in hybrid chromophoric surfactant amphiphile/silica nanocomposites. Angewandte Chemie International Edition 2006;45:1404–8.
[11] Tong H, Hong YN, Dong YQ, Ren Y, Häussler M, Lam JWY, et al. Color-tunable, aggregation-induced emission of a butterfly-shaped molecule comprising a pyran skeleton and two cholesteryl wings. The Journal of Physical Chemistry B 2007;111:2000–7.
[12] Dong Y, Lam JWY, Li Z, Tong H, Dong Y, Feng X, et al. Vapochromism of hexaphenylsilole. Journal of Inorganic and Organometallic Polymers and Materials 2005;15:287–91.
[13] Dong YQ, Lam JWY, Qin AJ, Sun JX, Liu JZ, Li Z, et al. Aggregation-induced and crystallization-enhanced emissions of 1,2-diphenyl-3,4-bis(diphenylmethylene)-1-cyclobutene. Chemical Communications; 2007:3255–7.
[14] Liu J, Lam J, Tang B. Aggregation-induced emission of silole molecules and polymers: fundamental and applications. Journal of Inorganic and Orgnometallic Polymers and Materials 2009;19:249–85.
[15] Hong Y, Lam J, Tang B. Aggregation-induced emission: phenomenon, mechanism and applications. Chemical Communications 2009;29:4332–53.
[16] Zhang W, Xie J, Yang Z, Shi W. Aggregation behaviors and photoresponsive properties of azobenzene constructed phosphate dendrimers. Polymer 2007;48:4466–81.
[17] Yao H, Morita Y, Kimura K. Effect of organic solvents on J aggregation of pseudoisocyanine dye at mica/water interfaces: morphological transition from three-dimension to two-dimension. Journal of Colloid and Interface Science 2008;318:116–23.
[18] Zhang Y, Xiang J, Tang Y, Xu G, Yan W. Aggregation behaviour of two thiacarbocyanine dyes in aqueous solution. Dyes and Pigments 2008;76:88–93.
[19] Jiang S, Zhang L, Liu M. Photo-triggered J-aggregation and chiral symmetry breaking of an anionic porphyrin (TPPS) in mixed organic solvents. Chemical Communications; 2009:6252–4.
[20] Yang Z, Chi Z, Yu T, Zhang X, Chen M, Xu B, et al. Triphenylethylene carbazole derivatives as a new class of AIE materials with strong blue light emission and high glass transition temperature. Journal of Materials Chemistry 2009;19:5541–6.
[21] Zhang X, Yang Z, Chi Z, Chen M, Xu B, Wang C, et al. A multi-sensing fluorescent compound derived from cyanoacrylic acid. Journal of Materials Chemistry 2010;20:292–8.
[22] Mongin O, Porrès L, Moreaux L, Mertz J, Blanchard-Desce M. Synthesis and photophysical properties of new conjugated fluorophores designed for two-photon-excited fluorescence. Organic Letters 2002;4:719–22.
[23] Danel K, Huang T, Lin JT, Tao Y, Chuen C. Blue-emitting anthracenes with end-capping diarylamines. Chemistry of Materials 2002;14:3860–5.
[24] Hu R, Lager E, Aguilar A, Liu J, Lam J, Sung H, et al. Twisted intramolecular charge transfer and aggregation-induced emission of BODIPY derivatives. The Journal of Physical Chemistry C 2009;113:15845–53.
[25] Chi Z, Yang Z, Zhang X, et al. Synthesis method and application of organic luminescent material containing carbazolyl stilbene derivative structure. Chinese Patent 2009, CN101343539.
[26] Hajime N, Chihaya A. Diphenyl ethane derivative and organic solid-state laser material using the same. Japanese Patent 2008, JP2008163190.
[27] Wang S, Oldham Jr WJ, Hudack Jr RA, Bazan GC. Synthesis, morphology, and optical properties of tetrahedral oligo(phenylenevinylene) materials. Journal of the American Chemical Society 2000;122:5695–709.
[28] Ning ZJ, Chen Z, Zhang Q, Yan YL, Qian SX, Cao Y, et al. Aggregation-induced emission (AIE)-active starburst triarylamine fluorophores as potential non-doped red emitters for organic light-emitting diodes and $Cl_2$ gas chemodosimeter. Advanced Functional Materials 2007;17:3799–807.
[29] Dong S, Li Z, Qin J. New carbazole-based fluorophores: synthesis, characterization, and aggregation-induced emission enhancement. Journal of Physical Chemistry B 2009;113:434–41.
[30] Tang B, Geng Y, Lam JWY, Li B, Jing X, Wang X, et al. Processible nanostructured materials with electrical conductivity and magnetic susceptibility: preparation and properties of maghemite/polyaniline nanocomposite films. Chemistry of Materials 1999;11:1581–9.
[31] Lechner M. Influence of Mie scattering on nanoparticles with different particle sizes and shapes: photometry and analytical ultracentrifugation with absorption optics. Journal of the Serbian Chemical Society 2005;70:361–9.
[32] Sun C, Zhou S, Chen P. Effects of different Hz sources on formation of J aggregation of cyanine dye. The Imaging Science Journal 2006;54:142–6.